Chemical Science International Journal

24(1): 1-20, 2018; Article no.CSIJ.43499
ISSN: 2456-706X
(Past name: American Chemical Science Journal, Past ISSN: 2249-0205)

Adsorption of 2,4-dinitrophenol on Activated Carbon Prepared from Cotton Cakes: Non-linear Isotherm Modeling

Bopda Aurelien[1], Tchuifon Tchuifon Donald Raoul[1], Nche George Ndifor-Angwafor[1], Kamdem Tamo Arnaud[2] and Anagho Solomon Gabche[1,3*]

[1]Research Unit of Noxious Chemistry and Environmental Engineering, Department of Chemistry, Faculty of Science, University of Dschang, P.O. Box 67, Dschang, Cameroon.
[2]Freiburg Materials Research Center (FMF), University of Freiburg, Stefan Meier Strasse 21, 79104 Freiburg, Germany.
[3]Department of Chemistry, Faculty of Science, University of Bamenda, P.B. Box 39 Bambili, Cameroon.

Authors' contributions

This work was carried out in collaboration between all authors. Authors BA, NGNA and ASG designed the study, performed the statistical analysis, wrote the protocol, and wrote the first draft of the manuscript. Authors TTDR and KTA managed the analyses of the study. Authors BA and TTDR managed the literature searches. All authors read and approved the final manuscript.

Article Information

DOI: 10.9734/CSJI/2018/43499
Editor(s):
(1) Dr. Pradip K. Bhowmik, Professor, Department of Chemistry, University of Nevada Las Vegas, USA.
Reviewers:
(1) Essy Kouadio Fodjo, Université Felix Houphouet Boigny, Cote d'Ivoire.
(2) Labidi Nouar Sofiane, University Centre of Tamanrasset, Algeria.
(3) Hidetaka Kawkaita, Saga University, Japan.
Complete Peer review History: http://www.sciencedomain.org/review-history/26294

Original Research Article

Received 24 June 2018
Accepted 12 September 2018
Published 19 September 2018

ABSTRACT

In this research, cotton cake has been investigated as a cheap and available precursor used for the production of novel carbon using phosphoric acid and potassium hydroxide as chemical activating agents with 2:1; 1:1, impregnation ratio at various concentrations of 0.5M; 1M; 1.5M using the batch adsorption mode to 2,4-dinitrophenol. Carbonization was performed at 450^{o}C for one hour and allowed to cool. The KOH activated carbon has exhibited high Iodine number values ranging

**Corresponding author: E-mail: sg_anagho@yahoo.com;*

between 447 and 590 mg/g. Thus, KOH was the activating agent in our study and the best ratio was used for the continuation of our work. The activated carbon was characterized by Fourier transform-infrared (FTIR) spectroscopy, scanning electron microscopy (SEM) and proximate analysis (pH_{ZCP}, pH, bulk density, moisture content, ash content, volatile mater, fix carbon content and matter soluble in water).The experimental isotherms were analyzed using two, three and four parameter sorption isotherm models. Three errors analysis methods were used to evaluate the experimental data: correlation coefficient (R^2), Chi-square (χ^2), Average Relative Error (ARE), Sum of Absolute Errors (EABS) and Root mean square error (RMSE) values were tested to find the best fitting isotherm. According to chi-square test (X^2), it appears that the Freundlich (two parameters), Hill (three parameters) and Marczweski-Jaroniec (four parameters) models describe better the adsorption data.

Keywords: Adsorption; 2,4-dinitrophenol; activated carbon; cotton cake; isotherms; error functions.

1. INTRODUCTION

Presently, the problem of pollution is becoming alarming increase in industrial activities. Concerns intensify by day, especially in terms of the contamination of drinkable water resources. In the last two decades, several research tasks were devoted to the description of the principal pollutants likely to increase the vulnerability of these resources. A report showed that phenol and its derivatives were dangerous pollutants. These residues came primarily from the rejection of pharmaceutical, polymeric, insecticidal industries. Among these compounds 2,4-dinitrophenol, is ranked by the US Environmental Protection Agency as being 121st out of the 275 most hazardous substances in terms of its toxicity [1]. The treatment of water contaminated by these classes of compounds are generally a difficult process. The presence of the nitro group in their structure provides them a strong chemical stability and resistance to microbial degradation [2]. Some physicochemical processes had been developed for the removal of phenolic compounds, including adsorption, extraction by chemical solvents, air stripping, freezing and crystallization, chemical oxidation, wet oxidation, and advanced oxidation processes [3,4].

Adsorption onto activated carbon is often considered as the most economical and efficient process for the removal of 2,4-dinitrophenol from diluted aqueous solutions because of its large surface area, controllable pore structure, high adsorption capacity, high purity, easy availability, thermal stability and functional groups. Some of the precursors such as Sugarcane bagasse [5], *Banana Empty Fruit Bunch and Delonixregia Fruit Pod* [6], *Fagopyrum esculentum* [7], coffee husks [8], rice husk [8,9]. Plant *Manihot Esculenta* [10], pistachio-nut shell [11], Cola Nut Shells [12] has been already used for activated carbon. The advantages of using agricultural by-products as raw materials for manufacturing activated carbon are; these raw materials are renewable and potentially less expensive to produce.

Adsorption isotherm data modeling is a valuable tool for predicting and comparing adsorption performance of various adsorbents. There are two, three, and four-parameters empirical isotherm models available for this purpose [13]. In recent years, the non-linear regression method has been proposed as a better way to find the best fitting of adsorption equilibrium. In the nonlinear regression method, the error distribution between the experimental data and the predicted isotherm must be minimized by an iterative procedure [14].

In this study, we have to examine nonlinear isotherms regression methods in detail and use these models to describe the adsorption 2,4-dinitrophenol by activated carbon obtained from cotton cakes.

2. MATERIALS AND METHODS

2.1 Materials

Processed cotton cake was collected from Zamay, Department of Mayo-Tsanaga, far Nord region of Cameroon [6]. They were cut into small pieces of about 0.5 to 1 cm in size, dried in sunlight until all the moisture evaporated.

2.1.1 Preparation of activated carbon

Preparation of activated carbon from cotton cake was carried out by chemical activation process with H_3PO_4 and KOH activating agents at different concentrations (0.5M; 1M and 1.5M). 120 grams of materials were inserted into each

five flasks of an activating agent solutions with impregnation ratios of 1/1, and 2/1, (w/w) were added to these flasks in order to activate the carbons. The mixture was allowed for 30 minutes for activation to take place before being dried up in an oven set at 105°C for 48 hours. The samples impregnated were carbonized for 1h at 450°C, at a heating rate of 5°C/min. After impregnation and carbonization, the pyrolyse carbons based KOH were leached with 1% HCl (v/v) for 2h and together with those from H_3PO_4, were washed several times with distilled water until a neutral pH for the two carbon based H_3PO_4 and KOH. Later, the carbon paste was dried in an oven at 110°C for at least 24 h and then converted to powder activated carbon with particle size slower than 100 µm and pestle before application. The prepared activated carbon was characterized by the adsorption capacity towards iodine, using the standard test method for the determination of iodine number of activated carbon (ASTM) for KOH and H_3PO_4 activation.

2.1.2 Characterization of activated carbons

The activated carbons were characterized by, Fourier transform-infrared (FTIR) spectroscopy, scanning electron microscopy (SEM), and proximate analysis (pH_{ZCP}, pH, Bulk density, moisture content, ash content, volatile mater, fix carbon content and matter soluble in water).

- **Iodine number:** To gain further knowledge of the porous structure of activated carbon, the adsorption of iodine from liquid phase was adopted by other researchers in the characterization of sludge-based activated carbons [15,16]. The adsorption of aqueous I_2 is considered a simple and quick test for evaluating the microporosity of activated carbons associated with pore diameter less than 2 nm. The iodine number, defined as the amount of iodine adsorbed per gram of activated carbon at an equilibrium concentration of 0.02 N, was measured according to the procedure established by the American Society for Testing and Materials [16]. Activated carbon of mass 0.1 g, was mixed with 30mL of 0.02N iodine solutions and stirred for 3 h. After filtration, 10 mL of the filtrate was titrated with 0.005N sodium thiosulphate solution using starch as indicator. The titration equation (1) is giving below

$$2\,Na_2S_2O_3\,(aq) + I2 \rightarrow Na_2S_4O_6\,(aq) + 2NaI\,(aq) \quad (1)$$

- **Water soluble matter:** 1 g of carbon sample was added to 100 mL of distilled water and stirred for about 30 minutes and then filtered. The residue was dried, cooled and weighed. Mass loss was calculated using Equation 2 [10].

$$\text{Water soluble matter}\,(\%) = \frac{\text{Mass of crucible with sample}\,(g) - \text{Mass of crucible after weight loss (g)}}{\text{Mass of crucible with sample}\,(g) - \text{Mass of crucible (g)}} X100 \quad (2)$$

- **Moisture content:** A previously weighed crucible was weighed with 1 g of powder, air dried activated carbon. It was then placed on a hot plate maintained at 110°C. It was taken out, cooled in a desiccator before being weighed again. The ratio of the mass lost per the powder to its original mass gave the moisture content of the sample [8,9].

- **Bulk Density:** A 25 cm^3 specific gravity bottle was weighed empty, and later when carefully filled to the mark with powder activated carbon. The difference in the masses gave the mass of the powder activated carbon [8,9]. The bulk density was calculated from the equation:

$$\text{bulk density} = \frac{\text{weight of powder}}{25} \quad (3)$$

- **Ash content/volatile matter [10,16]:** The standard test method for ash content-ASTM D2866-94 was used. A crucible was pre-heated in a muffle furnace to about 500°C, cooled in a desiccator and weighed. 1.0 g of activated carbon samples were transferred into the crucibles and reweighed. The crucibles containing the samples were then placed in a cold muffler furnace and the temperature was allowed to rise to 500°C. It was removed and allowed to cool in a desiccator to room temperature (25°C) and reweighed. The ash content was calculated using the equation.

$$\text{Ash}\,(\%) = \frac{Ash\ wheight\ (g)}{\text{Oven dry wheight}} X100 \quad (4)$$

Volatile matter was calculated using the equation;

$$\text{Volatile matter}\,(\%) = \frac{wheight\ of\ volatile\ \ component\ (g)}{\text{Oven dry wheight}} X10 \quad (5)$$

- **Fix carbon [10]:** The fixed carbon content is determined by subtracting the sum of percentage compositions of moisture content, the volatile matter content and the ash content from 100. The value obtained is the amount of fixed carbon present in the sample expressed as a percentage.

- **Determination of pH_{zcp}:** The pH of zero charge point of the activated carbons were carried out by adding 0.1 g of carbon to 30 mL solution of 0.1 M NaCl whose initial pH had been measured and adjusted with 0.1 M NaOH and 0.1M HCl varying between 2-10. The containers were sealed and placed on an agitator for 48 hours after which the pH was measured. The pHpzc occurs if there is no change in the pH after contact with adsorbent [16].

- **pH:** The pH of the activated carbons was determined by putting 50 mL of distilled water and 0.5 g of each of the carbons in different washed bottles. The mixtures were agitated for 24 h at room temperature. After, the mixtures were filtered and the pH of the filtrates was measured [8].

- **Boehm titration [12]:** The Boehm titration method was used for this analysis. 0.1 g of the activated carbon was added to a separate 50 mL solution of $NaHCO_3$ (0.1 M), Na_2CO_3 (0.1 M) and NaOH (0.1 M) for acidic groups and 0.1 M HCl for basic groups respectively at room temperature under agitation for 24 h. Subsequently, the aqueous solutions were back-titrated with HCl (0.1 M) and NaOH (0.1 M). The number and type of acidic sites were calculated by considering that NaOH neutralizes carboxylic, lactonic and phenolic groups, Na_2CO_3 neutralizes carboxylic and lactonic groups and that $NaHCO_3$ neutralizes only carboxylic groups. Carboxylic groups were therefore quantified by direct titration with $NaHCO_3$. The difference between the groups titrated with Na_2CO_3 and those titrated with $NaHCO_3$ was assumed to be lactones and the difference between the groups titrated with NaOH and those titrated with Na_2CO_3 was assumed to be phenol. Basic sites were determined by titration with HCl. In order to neutralize basic groups remaining HCl in the solution was back-titrated with 0.1 M NaOH.

2.1.3 Batch equilibrium experiments and analytical method

Stock solution of 2,4-dinitrophenol at the concentration of 500 mg/L was prepared by dissolving 0.250 g of sodium 2,4-dinitrophenol in 0.5 L of distilled water. Experimental solutions at desired concentrations were obtained by dilution of the stock solution with distilled water pre-adjusted to pH 2. The initial concentrations of the experimental solutions of 2,4-dinitrophenol were determined at 20, 25, 30, 35, 40, 45 and 50 mg/L. 30 mL of the experimental solutions were placed in bottles and then 0.05 g prepared activated carbon was added to each bottle. After agitation for about 2 h, the solution was filtered, and the filtrate analyzed to obtain the residual concentration 2,4-dinitrophenol by using the UV/Vis spectrophotometer at λ_{max} value of 320 nm.

2.2 Modelling Theoretical Background

Table 1 summarizes the non-linear forms of the two, three and four parameter isotherms models used in this study.

2.3 Error Functions Analysis

In general, when values of error function are low, it means there is an agreement between the experimental and calculated data and the model converges becomes favourable. Their error functions are listed in Table 2.

Table 1. Non-linear forms of the two, three and four parameter isotherms

Parameter	Isotherms	Non-linear forms	Reference
Two	Langmuir	$Q_e = \frac{Q_m K C_e}{1 + K C_e}$	[17]
	Freundlich	$Q_e = K_f C e^{1/n}$	[17]
	Dubinin-Radushkevich	$Q_e = Q_m \exp(-K\varepsilon^2)$; $\varepsilon = RT \ln(1+1/C_e)$;	[18]
	Temkin	$Q_e = Q_m \frac{RT}{\Delta Q} \ln(AC_e)$	[19]
	Jovanovic	$q_e = q_m(1 - e^{k_j C_e})$	[20]

Parameter	Isotherms	Non-linear forms	Reference
Three	Redlich-Peterson	$q_e = \frac{AC_e}{1 + BC_e^{\beta}}$	[21]
	Sips	$q_e = \frac{K_s C_e^{\beta}}{1 + a_s C_e^{\beta s}}$	[21]
	Toth	$\frac{q_e}{q_m} = \frac{K_e C_e}{[1 + (K_L C_e)^n]^{1/n}}$	[21]
	Hill	$q_e = \frac{q_{SH} C_e^{nH}}{K_D + C_e^{nH}}$	[21]
	Kahn	$Q_e = \frac{Q_{max} b_k C_e}{(1 + b_k C_e) a_k}$	[21]
Four	Fritz-Schlunder	$q_e = \frac{q_{mFSS} K_{FS} C_e}{1 + q_m C_e^{MFS}}$	[22]
	Baudu	$q_e = \frac{q_m bo C_e^{1+x+y}}{1 + bo C_e^{1+x}}$	[23]
	Marczewski-Jaroniec	$q_e = q_{MMJ}(\frac{(K_{MJ} C_e)^{n_{MJ}}}{1 + (K_{MJ} C_e)^{n_{MJ}}})^{M_{Mj}/n_{MJ}}$	[21]

Table 2. Error functions and their equations

Error function	Abbreviation	formula	Reference
Residual Root Mean Square Error	RMSE	$\sqrt{(\frac{1}{n-2}\sum_{i=1}^{n} q_{e,exp} - q_{e,calc}))^2}$	[24]
Hybrid fractional error function	HYBRID	$\frac{100}{n-p}\sum_{i=1}^{n}\frac{(q_{e,i,means} - q_{e,i,calc})^2}{q_{e,i,meas}}$	[23]
Average relative error	ARE	$\frac{100}{n-p}\sum_{i=1}^{n}\left(\frac{q_{e,i,calc} - q_{e,i,means}}{q_{e,i,meas}}\right)$	[25]
Nonlinear Chi-Square Test	**χ^2**	$\sum_{i=1}^{n}\frac{(q_{ecal} - q_{emeas})^2}{q_{emeas}}$	[26]
Sum of Absolute Errors	**EABS**	$\sum_{i=1}^{p}(q_{e,i,means} - q_{e,i,calc})$	[21]
coefficient of determination	**R^2**	$\frac{\sum_{i=1}^{n}(q_{ecal} - q_{mexp})^2}{\sum_{i=1}^{n}(q_{ecal} - q_{mexp})^2 + (q_{ecal} - q_{mexp})^2}$	[21]

3. RESULTS AND DISCUSSION

3.1 Characterization of Activated Carbons

3.1.1 Burn off and yield

The progress of the activation can be followed by the yield and the extent of "burn-off. The extent of burn-off of the carbon material is taken as a measure of the degree of activation. The burn-off of materials increases linearly with the total porous volume, which is directly related to the yield due to the reactions of activation of various biomasses used. Table 3 shows the burn-off and the yield of various carbons.

It is deduced from this table that the obtained yield in the process of activation of carbons obtained from cotton cake varies between 34-45% which indicates that activation resulting from a reaction of KOH and H_3PO_4 with the precursor, limits the burn-off of volatile matter. As such, Table 3 shows that the burn-off increases with decreasing yield, depending on the raw material. The values of burn-off ranges from 57 to 66 % indicating that these carbons have a structure of micro and mesopores [27].

3.1.2 Iodine number

In order to gain further knowledge of the porous structure of activated carbon, iodine adsorption from liquid phase was adopted by other researchers in the characterization of activated carbons. The adsorption of aqueous iodine is considered a simple and quick test for evaluating the surface area of activated carbons associated with pores larger than 1 nm [28]. Iodine number is an indication of the adsorption capacity in microspores. Therefore, it is often employed to examine the adsorption capacity of the activated carbons by researchers. Table 4 exhibits the iodine number of different activation carbons.

The results obtained by successive variation of the concentration of activating agents and the impregnation ratio on the production of activated carbons showed that: in the case of KOH, the iodine number increases with an increase in concentration. For H_3PO_4, a maximum is reached which is in order of 1M. These results confirm that chemical activation involves not only the creation of new pores, but also the widening of the pores available. Moreover, the type of activating agent used in the preparation of the activated carbon has an influence on the effectiveness of these carbons.

Table 4 shows that the activated carbon by KOH gave high Iodine number value ranging between 442 and 543 mg/g. These high values of the iodine number are due to the presence of a high microporosity, which could be explained by the reactivity of KOH. This microporosity is very low for the activated carbons prepared from H_3PO_4 with iodine numbers ranging between 228 and 320 mg/g. During the process of activation and carbonization, oxygen of the KOH could stabilize the carbon atoms crystallites. The potassium metal, obtained at the reaction temperature, can intercalate and force separately through the separate lamaelle of crystallite. The removal of potassium salts from the internal volume of carbon by washing creates microporosity in the activated carbon [29].

Table 3. Burn-off and yield of the chemical activation of the activated carbon using phosphoric acid and potassium hydroxide

Activating agent	Impregnation ratio	Concentration activating agent (M)	Y (%)	B (%)
KOH	1:1	0.5	37.43	62.57
		1.0	36.41	63.59
		1.5	36.30	63.70
	2:1	0.5	36.14	63.86
		1.0	35.90	64.10
		1.5	34.41	65.59
H_3PO_4	1:1	0.5	43.56	56.44
		1.0	43.76	56.24
		1.5	42.68	57.37
	2:1	0.5	44.54	55.46
		1.0	42.67	57.33
		1.5	42.31	57.69

Table 4. Iodine number of activation carbons

Activating agent	Impregnation ratios	Concentration activating agent (M)	Iodine number
KOH	1:1	0.5	494.91
		1.0	504.43
		1.5	523.46
	2:1	0.5	513.95
		1.0	523.46
		1.5	542.5
H_3PO_4	1:1	0.5	237.93
		1.0	295.05
		1.5	228.42
	2:1	0.5	352.15
		1.0	361.66
		1.5	276.01

Generally, the higher the iodine number, the greater the sorption capacity. ASTM D 4607 describes the procedure of determining the iodine number. The iodine number recommended as minimum by the American Water Works Association for a carbon to be used in removing low molecular weight compounds is 500. Thus, KOH is the best activating agent in our study and the best will be used for the continuation of our work. CCK1, CCK2 and CCK3 are obtained as follows:

- ✓ Cotton cakes to the Impregnation ratios 1:1 with the concentration 1.5 M (CCK1)
- ✓ Cotton cakes to the Impregnation ratios 2:1 with the concentration 1 M (CCK2)
- ✓ Cotton cakes to the Impregnation ratios 2:1 with the concentration 1.5 M (CCK3)

3.1.3 The proximate analysis

The proximate analysis was performed according to the ASTM methods. The proximate analysis for the determination of the pH, pH_{PZC}, Bulk density, matter soluble in water, volatile mater, ash content, moisture content and fixed carbon content was examined and show in Table 5.

The values of pH and pH_{PZC} of all the seven adsorbents are less than 7 and this shows that these absorbents have more acid groups on their surfaces. This result is according to Ahmedna et al. [30] and Okieimen et al. [31]. The bulk density of the prepared carbon is in the range between 464 and 618 (Table 3). The American Water Works Association (AWWA) has set a lower limit on the bulk density of 250 kg/m^3 for activated carbons to be of practical use [32]. The moisture content of all the activated carbons should be less than 5%. These results are in agreement with the set standards by American Water Works Association (AWWA). The low value of matter soluble in water was less than 0.5% indicating that all the carbons studied are almost insoluble in water and hence can be used for water analysis. This table shows that the ash content, volatile matter and fixed carbon content for these carbons are between 8 and 17%; 25 and 32; 55 and 59 respectively. One has low values of ash content and high value of fixed carbons. The ash content decrease while the volatile matter rates increase for these carbons. These results show that this material can be used as a good precursor to produce activated carbon [33]. From the data, it was clear that all the carbons have a good percentage of fixed carbon.

Fig. 1 shows the curve that determines the pH of the zero point charge.

3.1.4 Fourier transform Infra-red spectroscopy (FTIR)

The FTIR Analysis result showing the absorbance spectra of the cotton cake and activated carbon powder as shown in Fig. 2.

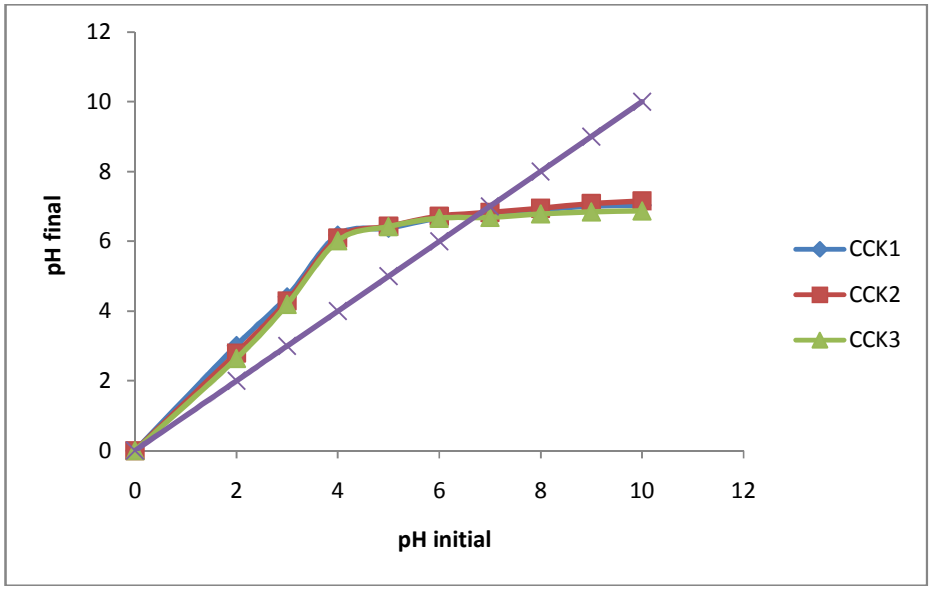

Fig. 1. Curve that determines the pH of the zero point charge

Table 5. The proximate analysis composition of CCK1, CCK2 and CCK3

Properties	CCK1	CCK2	CCK3
pH_{PZC}	6.55	6.58	6.47
pH	6.80	6.78	6.95
Bulk density (kg/m^3)	464.80	592.80	522.00
moisture content (%)	4.00	1.94	5.00
ash content (%)	16.20	11.00	8.20
volatile mater (%)	24.40	29.80	28.40
fixe carbon content (%)	55.40	57.26	58.40
matter soluble in water	0.35	0.30	0.28

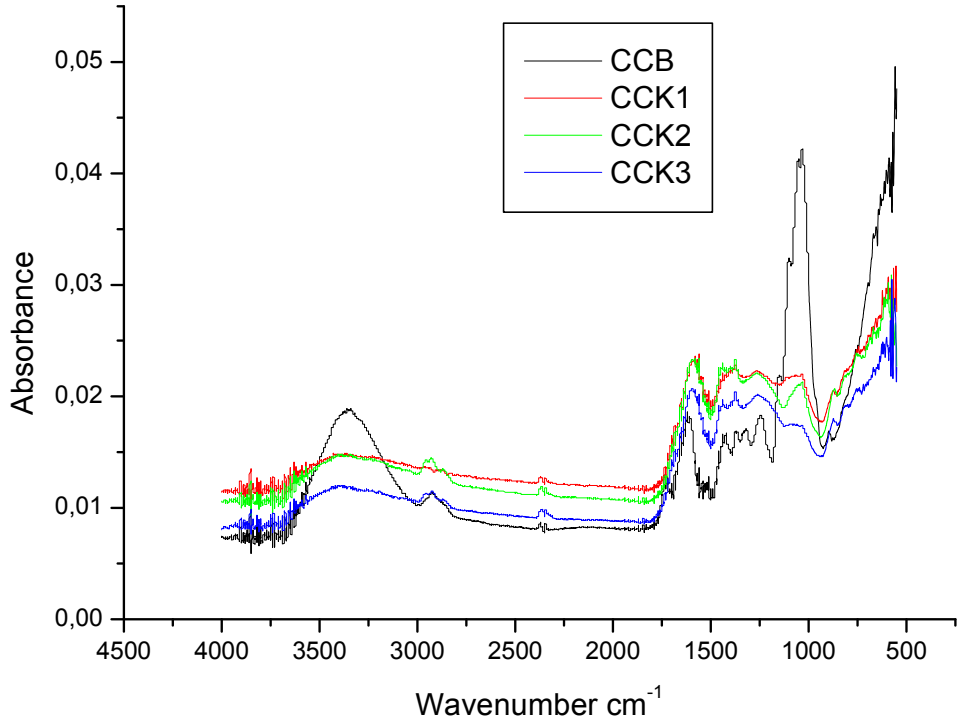

Fig. 2. Fourier transform infrared spectra of cotton cake and cotton cake based activated carbon

The FTIR Analysis result depicts the absorbance spectra of the cotton cakes powder. From Fig. 1, CCB spectra's vibrations implies the presence of either a free O-H or alcohol at the broad band with wave numbers between 3200 cm^{-1} to 3400 cm^{-1}. A vibration band at 3317 cm^{-1} was attributed to the presence of acetylenic stretching. The region between 2920 and 2550 cm^{-1} is assigned to C–H stretching vibrations. Also, 1605 cm^{-1} adsorption bands were attributed to quinonic, a monosubstituted alkene and carboxylate structures mean while the adsorption band of 1728 cm^{-1} was attributed to a carboxylic tautomeric structure (C=O). The bands located at 1100 and 1120 cm^{-1} are related to C-O stretching vibrations in alcohol and phenols [34]. Halogeno-alkanes could also be allocated at vibrations between 500 cm^{-1} and 800 cm^{-1}.

This behavior suggests that the activated carbon is mainly an aromatic polymer of activated carbon. The most important bands and peaks appearing on the spectrum of CCK1 are the same as presented on CCK2 and CCK3 but with low intensities of peaks O-H and C-H and that can be explained by the carbonization, which is at the origin of the atoms of C, O, H, in the form of CO_2, H_2O, aldehyde [35]. This comparison shows us an increase in the intensity of the peaks C-H and C=C of spectrum CCK1, CCK2 and CCK3 because of the elimination of the volatile mater by the carbonization process.

3.1.5 SEM analysis

The surface morphology of the activated carbons was studied by SEM techniques. The surface structures of the activated carbons have burnt out pores with tunnel or honeycomb-like structures as shown in Fig. 3.

Fig. 3 show that the adsorbent have rough texture with homogeneous surface and a variety of randomly distributed pore size. The surface of the activated carbons changed with impregnation ratios and concentration of activating agents. The SEM photographs for samples are characterized by a smooth surface with many orderly pores developed. This is as a result of lack of impurities such as tar that could clog up the pores and inhibit good pore structure development [36]. The development of large macropores on the particle surface can be appreciated when going from the carbonized raw material to the activated carbons CCK1, CCK2 and sample CCK3. However, the pores are non-uniform. During carbonization process, pores are developed in the carbon and promote the diffusion of KOH molecules into these pores and thereby increase the KOH–carbon reactions which would then create more pores in the activated carbon [29]. The external surface of the activated carbon is full of cavities with well-developed porous structure. The external surface shows a rough area having different pore diameters distributed over the surface of activated carbon. It seems that formation of cavity resulted from the removal of major components of raw materials and potassium hydroxide.

3.1.6 The boehm's titration results

Table 6 lists the amount of surface functional groups of activated carbon impregnated with KOH. A large amount of acidic groups such as carboxyl, phenolic, lactonic were detected on the adsorbents CCK1 and CCK2 while acidic group such as carboxyl is observed on the absorbents CCK3. These results are consisting with those of FTIR, pH and pH_{zcp}. The amount of acid groups was higher than the alkaline groups. The acid groups are beneficial for the ion exchange and electrostatic adsorption [12].

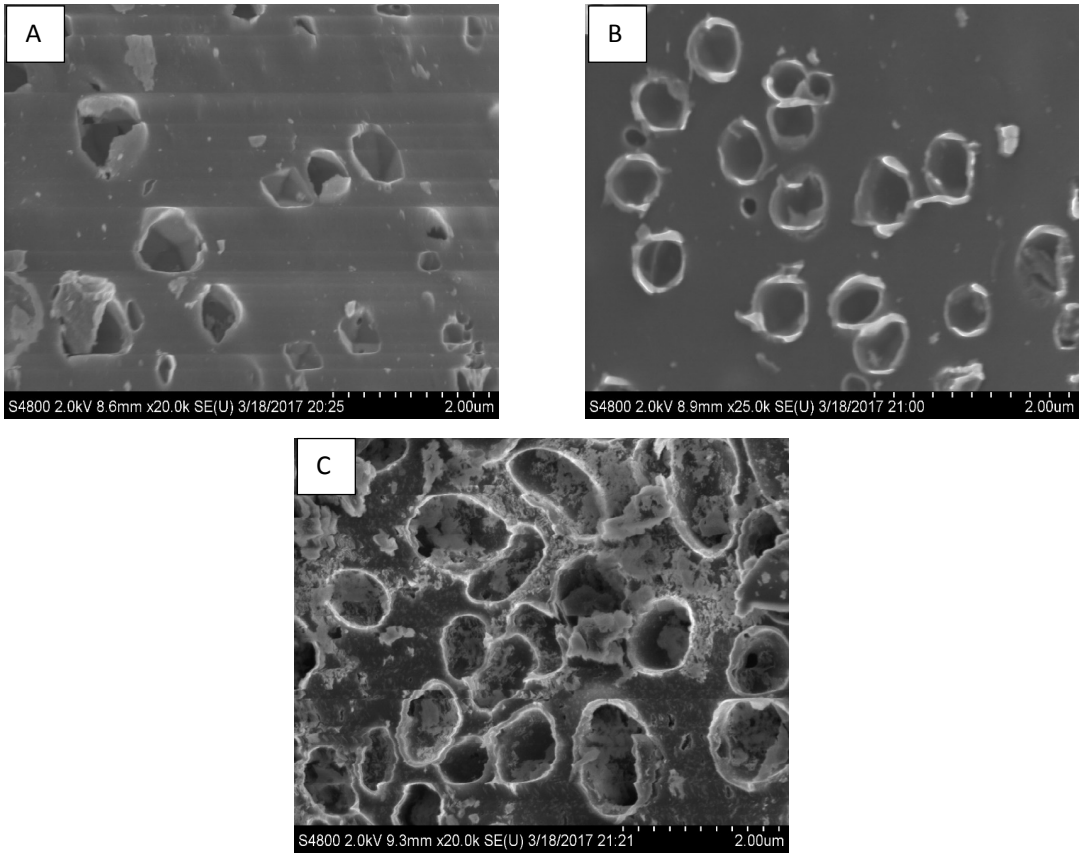

Fig. 3. SEM micrographs of activated carbon of samples: A) CCK1; B) CCK2 and C) CCK3

Table 6. Total acid and basic groups on surface of activated carbon

Functional groups	CCK1	CCK2	CCK3
Carboxylic groups (meq/g)	0.45	0.35	0.75
Lactonic groups (meq/g)	0.20	0.15	0.00
Phenolic groups (meq/g)	0.00	0.35	0.00
Total Acid group (meq g-1)	0.65	0.85	0.75
Total basic group (meq g-1)	0.45	0.45	0.55

3.2 Adsorption Isotherm Modelling onto CCK1, CCK2 and CCK3

In Non-linear regression method, the abilities of the widely used isotherms to model the equilibrium data were examined by a trial-and-error procedure using the *solver* add-in with Microsoft's spreadsheet, Microsoft Excel. The R^2 value is used to minimize the error distribution between the experimental equilibrium data and the predicted isotherms. To avoid such errors, we use the non-linear analysis as an adequate method. It is an interesting way for describing adsorption isotherms used for many applications such as wastewater treatment from industry. Figs. 4 to 12 show the fitting values of non-linear regression analysis. In addition, the error calculations are mentioned in Tables 7 to 9.

In this study, equilibrium data were fitted by five "two-parameter isotherms" (Langmuir, Freundlich, Temkin, Dubinin-Radushkevich, and Jovanovic) models, five "three-parameter isotherms"(Redlich-Peterson, Sips, Khan, Hill and Toth) and three four-parameter isotherms"(Fritz-Schlunder, Baudu and Marczewski-Jaroniec).

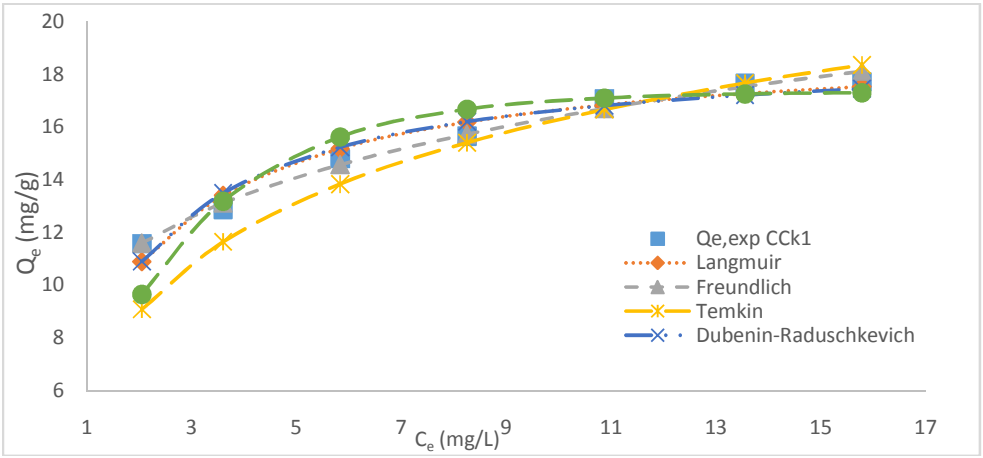

Fig. 4. Comparison of measured and calculated q_e values for two-parameter isotherms onto activated carbon CCk1

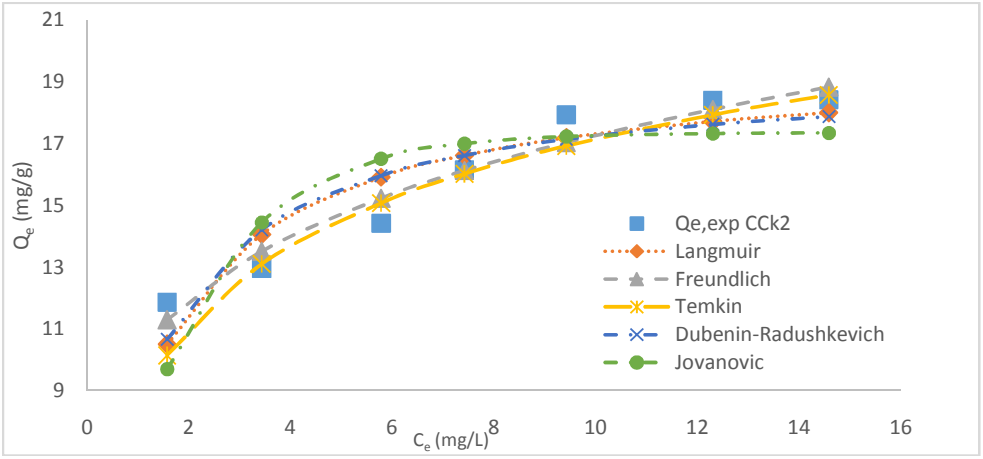

Fig. 5. Comparison of measured and calculated q_e values for two-parameter isotherms onto activated carbon CCk2

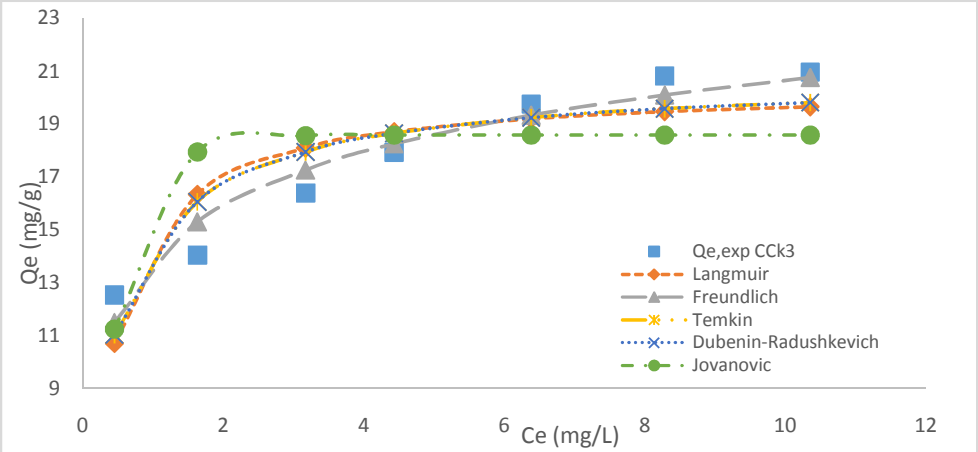

Fig. 6. Comparison of measured and calculated q_e values for two-parameter isotherms onto activated carbon CCk3

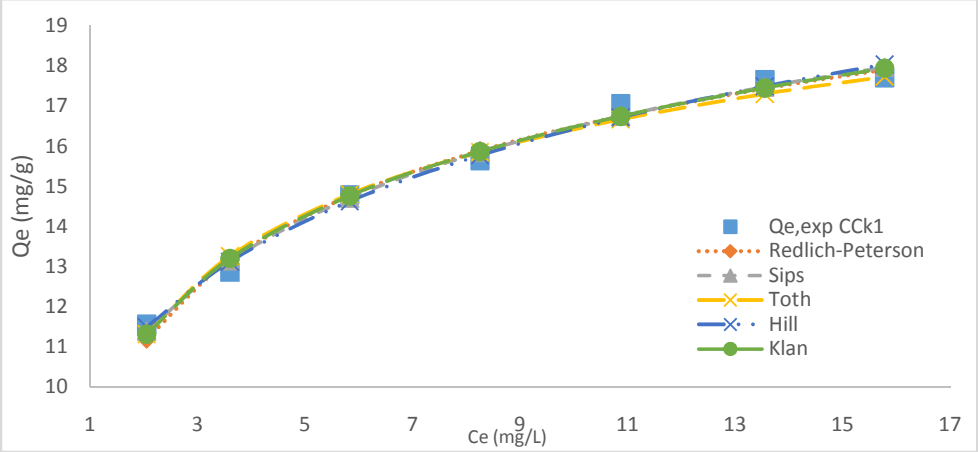

Fig. 7. Comparison of measured and calculated q_e values for three-parameter isotherms onto activated carbon CCk1

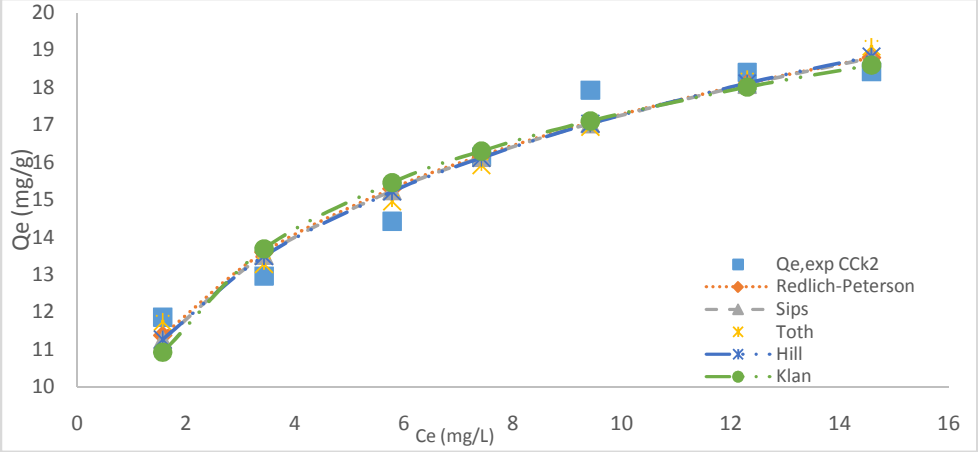

Fig. 8. Comparison of measured and calculated q_e values for three-parameter isotherms onto activated carbon CCk2

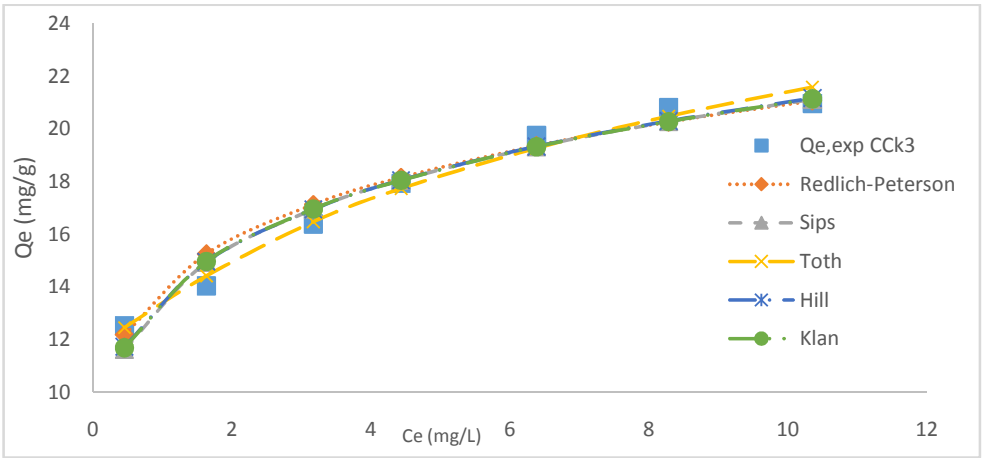

Fig. 9. Comparison of measured and calculated q_e values for three-parameter isotherms onto activated carbon CCk3

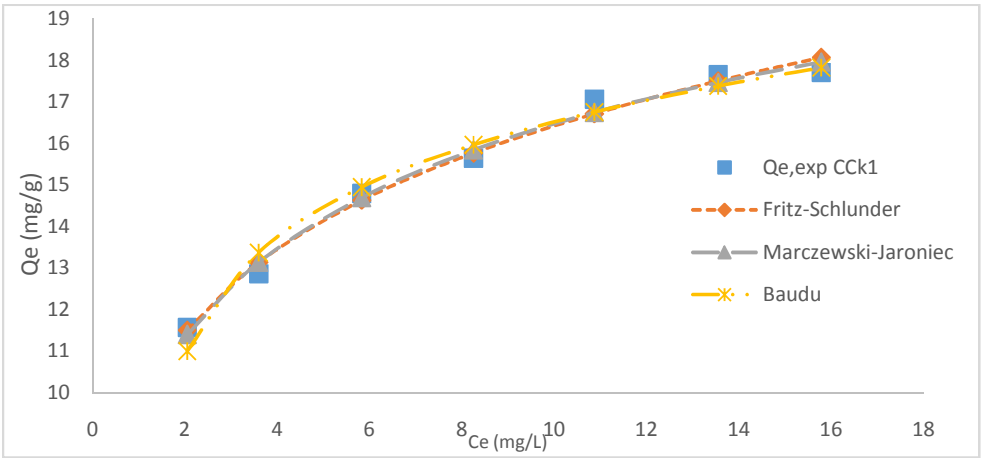

Fig. 10. Comparison of measured and calculated q_e values for four-parameter isotherms onto activated carbon CCk1

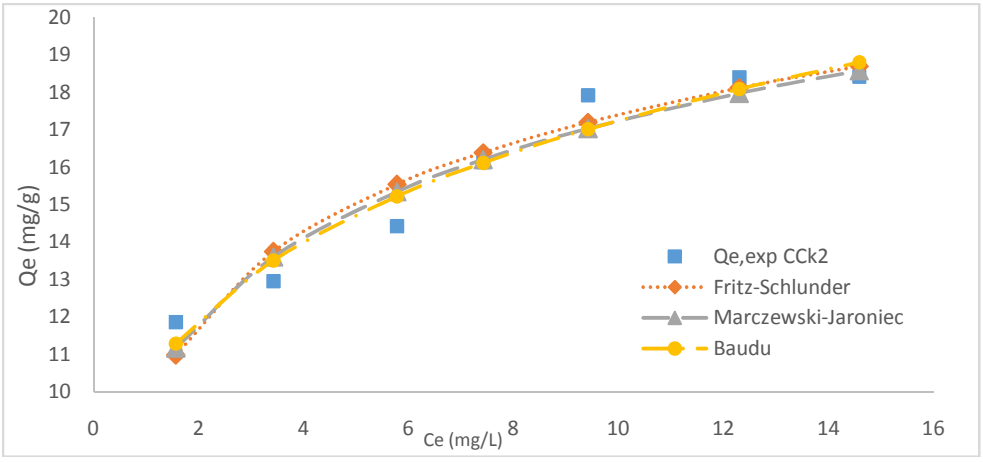

Fig. 11. Comparison of measured and calculated q_e values for four-parameter isotherms onto activated carbon CCk2

Table 7. Optimum isotherm parameters and their statistical comparison values for two-parameter models

N°	Models	Constants	Values	R^2	RMSE	χ^2	HYBRID	ARE	EABS
				CCK1					
1.	Langmuir	$\mathbf{Q_{max}}$ ($mg.g^{-1}$)	19.273	0.959	1.192	0.105	2.086	2.947	2.933
		$\mathbf{K_L}$ ($L.mg^{-1}$)	0.633						
2.	Freundlcih	$\mathbf{K_F}$ ($L.mg^{-1}$)	9.906	0.987	0.663	0.027	0.540	1.332	1.479
		n	4.575						
3.	Temkin	a ($L.mg^{-1}$)	3.609	0.994	3.044	0.915	15.036	5.015	5.972
		b ($J.mol^{-1}$)	546.02						
4.	Dubinin-Radushkevich	$\mathbf{Q_{max}}$ ($mg.g^{-1}$)	19.005	0.951	1.294	0.121	2.421	3.241	3.254
		K ($L.mg^{-1}$)	0.0002						
5.	Jovanovic	$\mathbf{Q_{max}}$ ($mg.g^{-1}$)	17.318	0.881	2.420	0.516	9.180	5.140	4.934
		$\mathbf{K_J}$ ($L.mg^{-1}$)	-0.397						
				CCK2					
1.	Langmuir	$\mathbf{Q_{max}}$ ($mg.g^{-1}$)	19.691	0.841	2.590	0.484	9.664	6.201	6.280
		$\mathbf{K_L}$ ($L.mg^{-1}$)	0.727						
2.	Freundlcih	$\mathbf{K_F}$ ($L.mg^{-1}$)	10.182	0.944	1.527	0.155	3.085	3.362	3.538
		n	4.360						
3.	Temkin	a ($L.mg^{-1}$)	9.281	0.912	2.163	0.396	7.026	4.266	4.264
		b ($J.mol^{-1}$)	654.58						
4.	Dubinin-Radushkevich	$\mathbf{Q_{max}}$ ($mg.g^{-1}$)	19.366	0.817	2.672	0.495	10.094	6.433	6.589
		K ($L.mg^{-1}$)	0.0002						
5.	Jovanovic	$\mathbf{Q_{max}}$ ($mg.g^{-1}$)	17.356	0.691	3.841	1.104	21.282	9.289	9.434
		$\mathbf{K_J}$ ($L.mg^{-1}$)	-0.521						
				CCK3					
1.	Langmuir	$\mathbf{Q_{max}}$ ($mg.g^{-1}$)	20.424	0.738	3.989	1.023	20.690	8.731	9.802
		$\mathbf{K_L}$ ($L.mg^{-1}$)	2.443						
2.	Freundlcih	$\mathbf{K_F}$ ($L.mg^{-1}$)	13.610	0.965	1.504	0.153	3.058	3.200	3.506
		n	5.291						
3.	Temkin	a ($L.mg^{-1}$)	108.57	0.932	2.059	0.283	5.709	4.409	4.824
		b ($J.mol^{-1}$)	838.56						

N°	Models	Constants	Values	R²	RMSE	χ²	HYBRID	ARE	EABS
4.	Dubinin-Radushkevich	Q_{max} (mg.g^{-1})	20.829	0.780	3.517	0.780	15.925	7.695	8.686
		K (L.mg^{-1})	0.0001						
5.	Jovanovic	Q_{max} (mg.g^{-1})	18.579	0.248	5.827	1.916	42.040	11.841	13.782
		K_J (L.mg^{-1})	-2.063						

Table 8. Optimum isotherm parameters and their statistical comparison values for three-parameter models

N°	Models	Constants	Values	R²	RMSE	χ²	HYBRID	ARE	EABS
			CCK1						
1.	Redlich-Peterson	**A** (L.g^{-1})	25.456	0.987	0.691	0.034	0.843	1.643	1.675
		B (L.mg^{-1})	1.966						
		β	0.866						
2.	Sips	K_s (L.g^{-1})	31.800	0.990	0.600	0.024	0.591	1.428	1.511
		a_s (L.g^{-1})	0.414						
		β_s	2.416						
3.	Toth	**Q** (mg.g^{-1})	13.051	0.983	0.746	0.038	0.937	1.611	1.664
		K_e	0551						
		n	0.935						
4.	Hill	Q_m (mg.g^{-1})	51.078	0.989	0.612	0.023	0.587	1.348	1.470
		K_H(L.g^{-1})	4.298						
		n_H	0.309						
5.	Khan	Q_m (mg.g^{-1})	10.352	0.987	0.659	0.030	0.739	1.552	1.612
		b_k (L.g^{-1})	2.340						
		a_k	0.841						
			CCK2						
1.	Redlich-Peterson	**A** (L.g^{-1})	511.645	0.941	1.549	0.158	3.983	3.404	3.580
		B (L.mg^{-1})	48.986						
		β	0.780						
2.	Sips	K_s (L.g^{-1})	152.034	0.943	1.544	0.159	3.968	3.401	3.564
		a_s (L.g^{-1})	0.071						
		β_s	3.927						
3.	Toth	**Q** (mg.g^{-1})	8.166	0.954	1.378	0.113	2.796	2.665	3.030
		K_e	-0.345						
		n	0.834						

N°	Models	Constants	Values	R^2	RMSE	χ^2	HYBRID	ARE	EABS
4.	Hill	Q_m ($mg.g^{-1}$)	2563.364	0.945	1.529	0.155	3.869	3.375	3.549
		K_H ($L.g^{-1}$)	251.617						
		n_H	0.232						
5.	Khan	Q_m ($mg.g^{-1}$)	10.545	0.922	1.836	0.240	5.971	4.192	4.249
		b_k ($L.g^{-1}$)	2.504						
		a_k	0.836						
			CCK3						
1.	Redlich-Peterson	**A** ($L.g^{-1}$)	110355	0.954	1.632	0.165	4.344	3.193	3.580
		B ($L.mg^{-1}$)	7879.0						
		β	0.825						
2.	Sips	K_s ($L.g^{-1}$)	144.61	0.963	1.562	0.168	4.156	3.309	3.600
		a_s ($L.g^{-1}$)	0.104						
		β_s	4.672						
3.	Toth	**Q** ($mg.g^{-1}$)	11.826	0.986	0.966	0.049	1.229	1.697	2.171
		K_e	-0.127						
		n	0.865						
4.	Hill	Q_m ($mg.g^{-1}$)	2264.1	0.965	1.508	0.153	3.835	3.215	3.525
		K_H ($L.g^{-1}$)	165.01						
		n_H	0.190						
5.	Khan	Q_m ($mg.g^{-1}$)	5.371	0.963	1.547	0.162	4.047	3.281	3.586
		b_k ($L.g^{-1}$)	156.65						
		a_k	0.815						

Table 9. Optimum isotherm parameters and their statistical comparison values for four parameter models

N°	Models	Constants	Values	R^2	RMSE	χ^2	HYBRID	ARE	EABS
			CCK1						
1.	Fritz-Schlunder	q_{mFS} ($mg.g^{-1}$)	34.130	0.988	0.630	0.025	0.829	1.367	1.492
		K_{FS} ($mg.g^{-1}$)	2.757						
		q_m ($mg.g^{-1}$)	8.860						
		M_{FS}	0.803						
2.	Marczewski-Jaroniec	q_{MMJ} ($mg.g^{-1}$)	28.132	0.990	0.594	0.023	0.767	1.412	1.498
		K_{MJ}	0.048						
		n_{MJ}	0.571						

N°	Models	Constants	Values	R^2	RMSE	χ^2	HYBRID	ARE	EABS
		M_{MJ}	0.330						
3.	Baudu	q_m (mg.g^{-1})	11.665	0.975	0.948	0.068	2.243	2.288	2.256
		b_0	1.392						
		x	0.887						
		y	0.155						
			CCK2						
1.	Fritz-Schlunder	q_{mFS} (mg.g^{-1})	16.939	0.922	1.841	0.239	8.050	4.272	4.326
		K_{FS} (mg.g^{-1})	2.006						
		q_m (mg.g^{-1})	2.632						
		M_{FS}	0.847						
2.	Marczewski-Jaroniec	q_{MMJ} (mg.g^{-1})	50.483	0.932	1.662	0.188	6.263	3.681	3.803
		K_{MJ}	2.069						
		n_{MJ}	0.231						
		M_{MJ}	0.615						
3.	Baudu	q_m (mg.g^{-1})	10.272	0.944	1.528	0.155	5.135	3.367	3.548
		b_0	115.27						
		x	-0.887						
		y	0.228						
			CCK3						
1.	Fritz-Schlunder	q_{mFS} (mg.g^{-1})	115.823	0.962	1.566	0.167	5.542	3.321	3.624
		K_{FS} (mg.g^{-1})	11.096						
		q_m (mg.g^{-1})	93.188						
		M_{FS}	0.817						
2.	Marczewski-Jaroniec	q_{MMJ} (mg.g^{-1})	138.913	0.958	1.654	0.186	6.200	3.487	3.781
		K_{MJ}	0.130						
		n_{MJ}	0.125						
		M_{MJ}	0.351						
3.	Baudu	q_m (mg.g^{-1})	16.413	0.965	1.504	0.153	5.097	3.200	3.506
		b_0	4.854						
		x	-1.000						
		y	0.189						

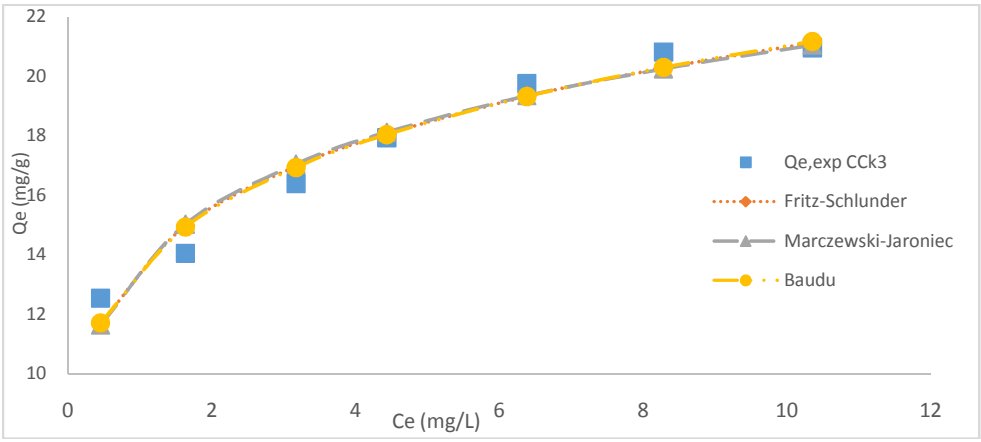

Fig. 12. Comparison of measured and calculated q_e values for four-parameter isotherms onto activated carbon CCk3

3.2.1 Two-parameter models

Table 7 shows the two isotherm parameters obtained using the Non-linear method. Higher values of R^2 obtained in this study are derived by fitting experimental data into the Temkin isotherm model for both CCK1 sample and Freundlich for both CCK2 and CCK3 samples. In addition, lower values of Chi-square (χ^2), ARE, EABS and Root mean square error (RMSE) for each parameter obtained in both isotherm models with higher R^2 can generate a satisfactory fit to the experimental data. As shown in Table 7, maximum adsorption capacity values obtained using non-linear Langmuir model, were 19.273, 19.691 and 20.424 mg/g for CCK1, CCK2, and CCK3 respectively. The values of n of the model of Freundlich are higher than 1 suggesting that the process occurred on heterogonous surfaces [17]. Based on the energies, the variation of energy of adsorption b (kJ/mol) resulting from the non-linearization of the Temkin model is positive. A positive value of b means that the process of adsorption is exothermic. From the Dubinin-Radushkevich model the adsorption energies are 42.25, 45.64 and 67.42 kJ/mol onto CCK1, CCK2 and CCK3 respectively, also high than 16 kJ/mol. These observations (values of energies) suggest that intra particular diffusion dominates the adsorption process. Jovanovic cannot describe the experimental equilibrium data because it is as a lower value of R^2 obtained in this study. In this study, all the values of error function are very small, indicating a favorable adsorption of 2,4-dinitrophenol on these different adsorbents.

3.2.2 Three-parameter models

Table 8 shows the three isotherm parameters obtained using the non-linear method. It was observed that the correlation coefficient value for all models isotherms study are very good (>0.94) with low Chi-square (χ^2), ARE, EABS and Root mean square error (RMSE) values, thus indicating that the models are able to describe equilibrium data perfectly. In the case of Slips model it shows high correlation coefficients value (0.99) for sample CCK1 and Toth model shows high correlation coefficients value (0.954, 0.986) respectively for CCK2 and CCK3 samples. Finally, they were chosen as the best fitted nonlinear model for data. These models are suitable for predicting adsorption on heterogeneous surfaces [21]. The adsorption maximum capacities determined for all samples using the Slips model are higher than those of Toth.

3.2.3 Four-parameter models

Table 9 shows the four isotherm parameters obtained using the Non-linear method. It was observed that the correlation coefficient value of all models isotherms study are very good (>0.93) and the low Chi-square (χ^2), ARE, EABS and Root mean square error (RMSE) values, thus it indicates that the models are able to describe equilibrium data perfectly. Higher values of R^2 obtained in this study are derived by fitting experimental data into the Marcewski-Jaroniec (0.99), Baudu (0.944) and Fritz-Schunder (0.965) isotherms model respectively for both CCK1 CCK2 and CCK3 samples. Finally, they were chosen as the best fitted nonlinear model for the data. These models are able to describe experimental data perfectly. Consequently, they were the most suitable models for this sorption system. The values of the maximum adsorption capacity obtained using all the three four

parameters isotherm are not according to those theoretical values calculated by the Langmuir.

4. CONCLUSION

A detailed analysis of the fits of several isotherm models to experimental adsorption equilibrium of 2.4-Diniphenol onto activated carbons prepared from cotton cakes was carried out. The activated carbons have burn-off higher to 55% showing a structure of micro and mesopores. The higher Iodine number of the activated carbon has been attributed to the presence of large micropore structure, which may be due to the reactivity of the activating agent KOH. The functional groups of the three carbons were determined using FTIR spectroscopy which was confirmed by using Boehm's titration. The best textural characteristics were obtained for the activation of carbonized cotton cakes with a KOH/carbon weight ratio of 2/1 with activating agent of 1.5M. Five two-parameter sorption isotherm models (Langmuir, Freundlich, Temkin, Dubinin-Radushkevich, and Jovanovic), five three-parameter models (Redlich-Peterson, Sips, Khan, Hill and Toth) and three four-parameter models (Fritz-Schlunder, Baudu and Marczewski-Jaroniec) were investigated from this analysis. The following conclusions are made based on the results obtained. Among CCK1, the Freundlich model (two parameter) better described the experimental data. The Toth model (three-parameter) was found to provide the best fit to the equilibrium experimental data for CCK2 and CCK3, because they have a high R^2, low Chi-square (χ^2), ARE, EABS and Root mean square error (RMSE) values. It was clear that both two-parameter Freundlich and three-parameter Toth isotherms were the best-fitting models for the experiment results (according to chi-square test (X^2)). This results explain the favorable adsorption of 2,4-dinitrophenol in these different adsorbents.

ACKNOWLEDGEMENTS

We grateful thank Professor Frank Marken (University of Bath) for his help and acknowledge technical assistance rendered by the researchers of Material and Process Engineering Team (MPET)/RUNOCHEE of the Department of Chemistry, Faculty of Science of the University of Dschang Cameroon.

COMPETING INTERESTS

Authors have declared that no competing interests exist.

REFERENCES

1. Murillo-Acevedo YS, Giraldo L, Moreno-Piraján JC. Characterization of the adsorption of 2,4-dinitrophenol from aqueous solution onto bovine bone char by immersion calorimetry. Adsorption Science & Technology. 2010;28:8-9.
2. Hutton EA, Ogorevc B, Hočevar SB, Weldon F, Smyth MR, Wang J. An introduction to bismuth film electrode for use in cathodic electrochemical detection. Electrochemistry Communication. 2001;3: 707-711.
3. Nadavala SK, Swayampakula K, Boddu VM, Abburi K. Biosorption of phenol and o-chlorophenol from aqueous solutions on to chitosan-calcium alginate blended beads. Journal of Hazardous Material. 2009;162: 482–489.
4. Rubin E, Rodriguez P, Herrero R, Sastre VME. Biosorption of phenolic compounds by the brown alga *Sargassum muticum*. Journal of Chemical Techonology and Biotechnology. 2006;81:1093–1099.
5. Quershi K, Bhatti I, Kazi R, Ansari AK. Physical and chemical analysis of activated carbon from sugarcane bagasse and use for sugar decolorization. World Academy of Science, Engineering and Technology. 2007;34.
6. Sugumarn P, Priya V, Susan P. Ravichandran, Seshadri S. Production and characterization of activated carbon from banana empty fruit bunch and delonixregia fruit pod. Journal of Sustainable Energy and Environ. 2012;3:125-132.
7. Kibami D, Chubaakum P, Rao KS, Sinha D. Preparation and characterization of activated carbon from *Fagopyrum esculentum* Moench by HNO_3 and H_3PO_4 chemical activation. Der Chemica Sinica. 2014;5(4):46-55.
8. Tchuifon TDR, Anagho SG, Ketcha JM, Ndifor-Angwafor GN, Ndi JN. Kinetics and equilibrium studies of adsorption of phenol in aqueous solution onto activated carbon prepared from rice and coffee husks. International Journal of Engineering and Technical Research. 2014;2:166-173.
9. Ndifor-Angwafor GN, Bopda A, Tchuifon TDR, Ngakou SC, Kuete TIH, Anagho SG. Removal of paracetamol from aqueous solution by adsorption onto activated carbon prepared from rice husk. Journal of Chemical and Pharmaceutical Research. 2017;9(3):56-68.

10. Pongener C, Kibami D, Rao K, Goswamee RL, Sinha D. Synthesis and characterization of activated carbon from the biowaste of the plant *manihot esculenta.* Chemical Science Transactions. 2015;4(1):59-68.
11. Yang T, Chong Lua A. Textural and chemical properties of zinc chloride activated carbons prepared from pistachio-nut shell. Materials in Chemistry and Physics. 2006;100:438-444.
12. Ndi JS, Ketcha JM, Anagho SG, Ghogomu JN, Bilibi EPD. Physical and chemical characteristics of activated carbon prepared by pyrolysis of chemically treated cola nut (cola acuminata) shells wastes and its ability to adsorb organics. International Journal of Advanced Chemical Technology. 2014;3:1-13.
13. Khan AR, Ataullah R, Al-Haddad A. Equilibrium adsorption studies of some aromatic pollutants from dilute aqueous solutions on activated carbon at different temperatures. Journal of Colloid and Interface Science. 1997;194:154–165.
14. Kumar VK. Optimum sorption isotherm by linear and non-linear methods for malachite green onto lemon peel. Dyes and Pigments. 2007;74:595-597.
15. Martin MJ, Artola A, Balaguer MD, Rigola M. Activated carbons developed from surplus sewage sludge for the removal of dyes from dilute aqueous solutions. Chemical Engineering Journal. 2003; 94(3):231-239.
16. ASTM International. Standard Test Method for Determination of Iodine Number of Activated Carbon: PA 19428-2959, United States,1 -5; 2006.
17. Al-Duri B, McKay G. Basic dye adsorption on carbon using a solid phase diffusion model. Chemical Engineering Journal. 1988;38(1):23-31.
18. Gunay A, Arslankaya E, Tosun I. Lead removal from aqueous solution by natural and pretreated clinoptilolite: Adsorption equilibrium and kinetics. Journal of Hazardous Material. 2007;146:362–371.
19. Ringot D, Lerzy B, Chaplain K, Bonhoure JP, Auclair E, Larondelle Y. In vitro biosorption of ochratoxin A on the yeast industry by-products: Comparison of isotherm models. Bioresource Technology. 2007;98(9):1812–1821.
20. Rania F, Yousef NS. Equilibrium and Kinetics studies of adsorption of copper (II) on natural Biosorbent. International Journal of Chemical/Engineering and Applications. 2015;6(5):319-324.
21. Ayawei N, Ebelegi AN, Wankasi D. Modelling and interpretation of adsorption isotherms. Journal of Chemistry. 2017;ID 3039817
22. Yaneva ZL, Koumanova BK, Georgieva NV. Linear regression and nonlinear regression methods for equilibrium modelling of p-nitrophenol biosorption by Rhyzopus oryzen: Comparison of error analysic criteria. Journal of Chemistry. 2013;1-10.
23. McKay G, Mesdaghinia A, Nasseri S, Hadi M, Aminabad MS. Optimum isotherms of dyes sorption by activated carbon: Fractional theoretical capacity and error analysis. Chemical Engineering Journal. 2014;251:236–247.
24. Subramanyam B, Das A. Linearized and non-linearized isotherm models comparative study on adsorption of aqueous phenol solution in soil. International Journal of Environmental Science & Technology. 2009;6(4):633-40.
25. Foo K, Hameed B. Insights into the modeling of adsorption isotherm systems. Chemical Engineering Journal. 2010; 156(1):2-10.
26. Chan L, Cheung W, Allen S, McKay G. Error analysis of adsorption isotherm models for acid dyes onto bamboo derived activated carbon. Chinese Journal of Chemical Engineering. 2012;20(3):535-42.
27. Bansal RC, Donne JB, Stoeckli F. Active Carbon", Marcel Dekker, Inc, New York; 1988.
28. Benadjemia M, Milliere RL, Benderdouche N, Duclaux L. Preparation, Characterization and Methylene blue adsorption of phosphoric acid activated carbons from globe artichoke leaves. Fuel Processing Technology. 2011;92:1203-1212
29. Sahira J, Bhadra PP. Preparation and characterization of activated carbon from lapsi (*Choerospondias axillaris*) seed stone by chemical activation with potassium hydroxide. Journal of the Institute of Engineering. 2013;9(1):79–88.
30. Ahmedna M, Marshall WE, Rao RM. Granular activated carbons from agricultural by–products: preparation properties and application in cane sugar refining. Bulletin of Louisana State University Agricultural Centre. 2000; 54.

31. Okieimen FE, Okiemen CO, Wuana RA. Preparation and characterization of activated carbon from rice husks. Journal of Chemical Society. 2007;32:126-136.
32. Omlin J, Cheseaux L. Evaluation des charbons actifs en poudre (CAP) pour l'élimination des micropolluants dans les eaux urbaines. Rapport d'étude, Ecole Polytechnique Fédérale de Lausanne, Lausanne, France. 2010;62.
33. Prahas D, Kartika Y, Indraswati N, Ismadji S. Activated carbon from jackfruit peel waste by H_3PO_4 chemical activation: Pore structure and surface chemistry characterization. Chemical Engineering Journal. 2008;140:32–42.
34. Virote B, Srisuda S, Wiwut T. Preparation of activated carbons from coffee residue for the adsorption of formaldehyde. Separation and Purification Technolgy. 2005;42:159–168.
35. Ndi JN, Ketcha MJ The adsorption efficiency of chemically prepared activated carbon from Cola Nut Shells by $ZnCl_2$ on methylene Blue. Journal of Chemistry. 2013;ID 469170:1-7.
36. Abechi SE, Gimba CE, Uzairu A, Dallatu YA. Preparation and characterization of activated carbon from palm kernel shell by chemical activation. Research Journal of Chemical Sciences. 2013; 3(7):54-61.

Peer-review history:
The peer review history for this paper can be accessed here:
http://www.sciencedomain.org/review-history/26294